Expression, immunogenicity and clinical significance analysis of thyroid-stimulating hormone receptor fusion proteins

XIA CHEN and HUI CHEN

Department of Endocrinology and Metabolism, The Second Hospital and Clinical Medical School, Lanzhou University, Lanzhou, Gansu 730000, P.R. China

Received November 30, 2024; Accepted April 16, 2025

DOI: 10.3892/mmr.2025.13639

Abstract. Thyroid function is regulated in a substantial manner by thyroid-stimulating hormone receptor (TSHR), and aberrant alterations in thyroid function are triggered by the interaction of TSHR with its antibodies, thyroid-stimulating hormone receptor antibodies (TRAb). The expression, immunogenicity and clinical significance of fusion proteins comprising different structural domains of TSHR were investigated. Fusion proteins containing several human TSHR (hTSHR) structural domains were created. *In vitro* experiments utilized these fusion proteins as antigens to specifically bind and analyze patient sera using an ELISA. To investigate the immunogenicity and clinical significance of various structural domains of TSHR, *in vivo* experiments included immunizing BALB/c mice with various fusion proteins of hTSHR, measuring serum autoantibodies, assessing thyroid function, performing histological examination and using flow cytometry to identify changes in T cell subsets. Three distinct hTSHR fusion protein fragments (hTSHR289, hTSHR290 and hTSHR410) were synthesized. The hTSHR290 fusion protein demonstrated the highest binding reaction with $TRAb^+$ sera from patients with hypothyroidism, and the hTSHR289 fusion protein demonstrated considerable specific binding reactivity with stimulating antibodies, as observed in sera from patients with hyperthyroidism. Pathological alterations associated with hyperthyroidism were observed in mice in the hTSHR289 fusion protein group, while pathological changes associated with hypothyroidism were observed in mice in the hTSHR290 fusion protein group. Immunized BALB/c mice exhibited increased levels of $CD4^+$ T cell subsets, and decreased levels of $CD8^+CD122^+$ and $CD4^+CD25^+$ T cell subsets. Fusion proteins of different structural domains of TSHR exhibited varying immunogenicity. The hTSHR289 fusion protein and hTSHR290 fusion protein prepared in the present study could serve as a basis for the development of ELISA kits for the detection of thyroid-stimulating immunoglobulins and TSHR-blocking antibodies. Fusion proteins of different structural domains of TSHR induced clinical symptoms of hyperthyroidism and hypothyroidism in mice. The present study provides a scientific basis for future studies on the etiology and mechanisms of autoimmune thyroid diseases, as well as the invention of novel methods for TRAb detection.

Correspondence to: Professor Hui Chen, Department of Endocrinology and Metabolism, The Second Hospital and Clinical Medical School, Lanzhou University, 82 Cuiyingmen, Chengguan, Lanzhou, Gansu 730000, P.R. China
E-mail: chenhui@lzu.edu.cn

Key words: thyrotropin receptor, fusion protein, thyroid-stimulating hormone receptor antibodies, immunogenicity, autoimmune thyroid diseases

Introduction

Graves' disease (GD), Hashimoto's thyroiditis (HT) and other autoimmune thyroid diseases (AITDs) are organ-specific autoimmune diseases that are more common than type 1 diabetes and multiple sclerosis (1). The thyroid-stimulating hormone receptor (TSHR), as a G protein-coupled receptor (GPCR), serves a key role in regulating thyroid function (2). Specific autoantibodies such as thyroid-stimulating hormone receptor antibodies (TRAb) bind to TSHR, inducing abnormal changes in thyroid function, which are the fundamental causes of diseases such as GD and HT (3).

TSHR autoantibodies have stimulatory thyroid-stimulating immunoglobulins (TSAb) that block TSHR-blocking antibodies (TBAb) or neutral activity, and the different activities of TRAb are associated with the progression of AITDs, leading to the occurrence of clinically relevant diseases. TSAb serves a key role in the development of GD, as it activates the adenylyl cyclase signaling system upon binding with TSHR, leading to an abnormal elevation of thyroid hormones (4). Additionally, TSAb is not controlled by the physiological hypothalamic-pituitary-thyroid negative feedback loop. After TSAb binds to TSHR, it causes the activation of the cAMP pathway and the secondary activation of inositol 1,4,5-triphosphate, which promotes the proliferation of thyroid follicular cells and the excessive synthesis and secretion of thyroxine, and ultimately leads to the pathogenesis of GD (5). However, TBAb blocks the binding of thyroid-stimulating hormone (TSH) to TSHR, causing hypothyroidism and subsequently inducing HT (6). The serum TRAb positivity rate reaches 80-90% in patients with newly diagnosed GD, and as treatment progresses, TRAb titers change accordingly (5). The different

activities of TRAb are associated with the progression of AITDs, leading to the interconversion between hyper- and hypothyroidism (7). At present, it is difficult to distinguish and differentiate TSAb from TBAb in clinical tests, which makes clinical diagnosis and treatment difficult. This also poses challenges in monitoring the disease progression of a patient and providing precise treatment (8). Therefore, it is key to differentiate the active types of TRAb in the diagnosis and treatment of autoimmune diseases, such as GD, HT and mucinous edema.

Different methods of detecting TRAb are being investigated. Currently, competitive binding assays and bioassays are used for TRAb detection. However, these binding assays cannot distinguish between TSAb and TBAb, while bioassays measure the functional activity of TRAb rather than simple binding (8). As a result, compared with binding assays, bioassays can more accurately detect the different activities of TRAb. However, bioassays are complex and time-consuming, requiring the use of experimental equipment and technicians to conduct cell experiments, so cannot be widely used in clinical testing (9). Since TSHR is the main autoantigen in the pathogenesis of GD and HT [particularly the extracellular region of TSHR, which is the cluster region of antigenic determinants, with the A subunit of TSHR being the binding site for TSAb (10), and the B subunit of TSHR being the binding site for TBAb, the interaction between TSHR and thyroid-specific lymphocytes and TRAb induces the occurrence and development of AITD (11). Therefore, analysing the characteristics of AITD induced by the combination of different domains of TSHR and its autoantibodies may provide a novel approach for precise diagnosis, treatment and prevention for patients.

Given the key role of TSHR and its antibody, TRAb, in the occurrence, development and prognosis of AITDs, studies have been conducted using cloning, sequence analysis and partial crystallization to confirm that TSHR possesses unique structural and functional characteristics (12-14). TSHR is composed of extracellular domains (ECDs) and transmembrane domains (TMD) involved in membrane-bound signal transduction (15,16). The ECD structure contains leucine-rich repeat domains [LRRDs; amino acid (aa)22-279], which are rich in leucine (16). The molecular activation mechanism of TSHR differs from that of other GPCRs, as its ECD (aa1-418) is larger and primarily responsible for specific binding with TSH and TRAb. The binding of TRAb or TSH to TSHR can trigger conformational changes in the ECD, and TSAb or TBAb can only bind to the ECD when the spatial conformation of TSHR is correct. This interaction affects thyroid function and induces a cascade of signal transduction via TMD leading to the development of AITD (17,18). Therefore, understanding the antigenic epitopes involved in the binding of TSHR to TSAb and TBAb helps clarify the pathogenic mechanisms of GD, HT and other related autoimmune diseases. In the present study, different fragments of the TSHR ECD were designed to simulate their natural activity through the preparation of fusion proteins. The pathogenic antigenic epitopes of TSHR and their immunogenicity were explored in both *in vitro* and *in vivo* experiments, with the aim of understanding the specific binding sites between TSHR and its pathogenic antibodies. The present study provided a scientific basis for the development of detection methods for different types of TRAb, the construction of disease animal models, and the diagnosis and treatment of GD, HT and associated autoimmune diseases.

Materials and methods

Serum samples and study population. In the present study, a total of 120 patients (aged 18-56 years) and 30 healthy individuals (aged 18-52 years) were recruited between January 2023 and January 2024 from The Second Hospital and Clinical Medical School of Lanzhou University (Lanzhou, China). Thyroid assessments were conducted for all participants based on the guidelines outlined in 'Thyroid disease: assessment and management' [National Institute for Health and Care Excellence (NICE) guideline NG10074] released by NICE in 2019 (19). The assessments included the medical history, clinical symptoms, physical examinations, thyroid ultrasound and thyroid function tests [TSH, free triiodothyronine (FT3) and free thyroxine (FT4)]. The exclusion criteria included acute or chronic infections, other autoimmune or chronic diseases, malignancies, hepatic or renal dysfunction, pregnancy, lactation or the use of glucocorticoids, antibiotics, and interferons or other medications affecting the immune system and thyroid function.

The 120 patients were divided into four groups based on their levels of TRAb [serum TRAb levels >1.5 IU/l measured by chemiluminescence were considered to be positive. By combining TRAb in serum with the TSHR-biotin-streptavidin-magnetic bead complex (cat. no. 88817; Thermo Fisher Scientific, Inc.) and then with the alkaline phosphatase-labeled anti-human IgG secondary antibody (cat. no. PA1-85606; Thermo Fisher Scientific, Inc.; 1:10,000; diluted in PBS; 2 h at room temperature)], chemiluminescence is produced. The intensity of the chemiluminescence signal is positively associated with the concentration of TRAb): 30 patients with hyperthyroidism who were $TRAb^+$ (age, 33.91±13.06 years; 10 male and 20 female patients), 30 patients with hyperthyroidism who were $TRAb^-$ (age, 35.10±13.76 years; 9 male and 21 female patients), 30 patients with hypothyroidism who were $TRAb^+$ (age, 33.17±18.97 years; 11 male and 19 female patients), 30 patients with hypothyroidism who were $TRAb^-$ (age, 37.4±16.86 years; 10 male and 20 female patients). Furthermore, 30 healthy individuals were included as the control group (age, 34.9±12.23 years; 12 male and 18 female patients).

All patients were newly diagnosed and did not receive any treatment, and all subjects had no thyroid nodules, thyroid cancer or other thyroid changes. Individuals with other complicating diseases, extrathyroidal manifestations or who received medications such as steroids that may affect immune function or thyroid function were excluded from the present study. The research protocol was reviewed and approved by the Medical Ethics Committee of The Second Hospital of Lanzhou University (approval no. 2023A-802; Lanzhou, China). All participants provided written informed consent prior to participating in the present study.

Thyroid function and thyroid-specific autoantibody testing. Fasting whole blood samples were collected from all participants after an 8-h fast. Samples were analyzed at the Department of Nuclear Medicine, Second Hospital of Lanzhou

Table I. Primer sequences.

Gene	Forward primer	Reverse primer
hTSHR410	5'-CACCGGAATGGGGTGTTCGTCTCC-3'	3'-CACAATTCTCAGGAACTTGTAGCCCA-5'
hTSHR290	5'-CACCAAGAAAATCAGAGGAATCCT-3'	3'-CACAATTCTCAGGAACTTGTAGCCCA-5'
hTSHR289	5'-CACCATGAGGCCGGCGGA-3'	3'-CTGATTCTTAAAAGCACAGCAGTGGC-5'

aa, amino acid; hTSHR, human thyroid-stimulating hormone receptor.

University (Lanzhou, China), using a chemiluminescence immunoassay to assess the levels of TSH (cat. no. 06491080; Siemens Healthineers), FT3 (cat. no. 119781; Siemens Healthineers), FT4 (cat. no. 06490106; Siemens Healthineers), TG (cat. no. 11201760; Siemens Healthineers), TPOAb (cat. no. 10630887; Siemens Healthineers) and TRAb (cat. no. 130203009M; Shenzhen New Industries Biomedical Engineering Co., Ltd.) in the serum. The kits were all used according to the manufacturer's instructions.

Cloning of the human TSHR (hTSHR) recombinant gene. The hTSHR gene sequence, protein amino acid sequence and spatial structural characteristics were determined by querying the Uniprot (https://www.uniprot.org/) and National Center for Biotechnology Information (https://www.ncbi.nlm.nih.gov/) databases. Primers were designed using Primer 3.0 (https://primer3.ut.ee/) according to the Champion™ pET vector connection requirements and synthesized by Sangon Biotech Co., Ltd. (Table I). The hTSHR plasmid, preserved by the Endocrinology and Metabolism Laboratory of Lanzhou University Second Hospital, and PrimeSTAR® HS DNA polymerase [Takara Biomedical Technology (Beijing) Co., Ltd.] were used for PCR amplification of the target gene. PCR primer (5'-3') sequences were as follows: hTSHR410 forward, CACCGGAATGGGGTGTTCGTCTCC and reverse, CAC AATTCTCAGGAACTTGTAGCCCA; hTSHR290 forward, CACCAAGAAAATCAGAGGAATCCT and reverse, CAC AATTCTCAGGAACTTGTAGCCCA; and hTSHR289 forward, CACCATGAGGCCGGCGGA and reverse, CTG ATTCTTAAAAGCACAGCAGTGGC. The following thermocycling conditions were used: 98˚C for 5 min, followed by 30 cycles of 98˚C for 10 sec, 55˚C for 5 sec and 72˚C for 30-90 sec; 72˚C for 5 min, followed by a 4˚C hold. PCR experiments were performed using the T100 Thermal Cycler (Bio-Rad Laboratories, Inc.). Gene size was determined by 2% agarose gel electrophoresis (visualization method, green fluorescent nucleic acid dye; cat. no. G8140; Beijing Solarbio Science & Technology Co., Ltd.) and imaging (BluSight Pro; GD50502; Monad Biotech Co., Ltd.), and the purified gene was extracted using the Gene JET Gel extraction kit (Invitrogen; Thermo Fisher Scientific, Inc.). The gene concentration was determined using a UV spectrophotometer. According to the Champion™ pET102 Directional TOPO™ Expression Kit (Invitrogen; Thermo Fisher Scientific, Inc.) requirements, the purified and recovered hTSHR target gene was connected to pET102-D-TOPO and transformed into competent TOP10 cells [Invitrogen; Thermo Fisher Scientific, Inc.; TOP10 *Escherichia coli* cells were cultured in S.O.C. medium (Thermo Fisher Scientific, Inc.) supplemented with 100 μg/ml ampicillin (Beijing Solarbio Science & Technology Co., Ltd.) at 37˚C] by adding 3 μl reaction mixture to 50 μl TOP10 cells (Invitrogen; Thermo Fisher Scientific, Inc.). The recovered bacterial liquid was spread onto LB (Beijing Solarbio Science & Technology Co., Ltd.) solid plates containing 100 μg/ml ampicillin and incubated overnight at 37˚C.

Monoclonal colonies were picked out from the petri dish, the picked colonies were mixed in sterile and enzyme-free water, and then PCR was performed under the aforementioned PCR reaction conditions. They were confirmed and identified using 2% agarose gel electrophoresis (visualization method, green fluorescent nucleic acid dye; cat. no. G8140; Beijing Solarbio Science & Technology Co., Ltd.) and imaging (BluSight Pro; GD50502; Monad Biotech Co., Ltd.). Positive colonies were inoculated into LB liquid medium (Beijing Solarbio Science & Technology Co., Ltd.) with 100 μg/ml ampicillin (Beijing Solarbio Science & Technology Co., Ltd.) and shaken overnight (37˚C; 220 rpm), and plasmids were extracted from recombinant TOP10-hTSHR cells using a plasmid mini-prep kit (TIANprep Mini Plasmid Kit; cat. no. DP103; Tiangen Biotech Co., Ltd.) according to the manufacturer's instructions.

After collecting the bacteria, using the plasmid mini-prep kit, Buffer P1 solution, Buffer P2 solution and Buffer P3 solution containing RNaseA were added sequentially, and the supernatant was moved into the adsorption column CP3 and centrifuged for 2 min at room temperature at 13,400 x g, and the elution buffer EB was added dropwise to the middle part of the adsorption membrane, and the recombinant plasmid solution containing the target gene was collected into the centrifuge tube after centrifugation for 2 min at room temperature at 13,400 x g. Using a 3730xl DNA Analyzer (cat. no. A41046; Thermo Fisher Scientific Inc.), the extracted recombinant plasmid was used as a template, and the primers used were: Forward, TTCCTCGACGCTAACCTG and reverse, TAGTTATTGCTCAGCGGTGG. In the 3730xl DNA Analyzer, the plasmid to be tested first replicates DNA from the primer under the catalysis of DNA polymerase until the reaction stops when it encounters ddNTP. Then, the sequence of the DNA obtained from the reaction is read by gel electrophoresis, and ultimately the gene sequence of the plasmid to be tested is inferred (Sequencing Analysis v7.1; Thermo Fisher Scientific Inc.).

Transformation of different hTSHR recombinant plasmids into Escherichia coli for expression. Each TOP10-hTSHR recombinant plasmid was transformed into *Escherichia coli* BL21Star™ (DE3) (Invitrogen; Thermo Fisher Scientific, Inc.).

Following expansion culture, induction of hTSHR fusion protein expression was carried out using 0.5 mmol/l isopropyl β-D-1-thiogalactopyranoside (IPTG). After 5 h of induction at 25˚C, the bacterial culture was collected. The cells were resuspended in 1X PBS or binding buffer (20 mM sodium phosphate; 0.5 M NaCl; 5 mM imidazole; pH 7.4). The cells were disrupted using a cell disruptor, and the bacterial lysate was centrifuged at 13,400 x g for 20 min at 4˚C to collect the supernatant and pellet. SDS-PAGE was conducted to determine the expression of each hTSHR fusion protein, distinguishing between expression in the supernatant and inclusion bodies. A total of 10 ng of protein was loaded per lane in a 10% gel.

Expression and purification of hTSHR recombinant protein. Expression and purification of the hTSHR fusion protein, tagged with histidine (His), were performed using a Nickel-nitrilotriacetic acid (Ni-NTA) column. The process involved collecting precipitated bacteria from LB culture following IPTG induction. The collected cells were sonicated on ice (ultrasonic power 200 W; 40 min), and the resulting mixture was subjected to low-temperature centrifugation at 13,400 x g for 20 min at 4˚C to separate the precipitate and supernatant. The inclusion bodies in the precipitate were dissolved in binding buffer (20 mM sodium phosphate; 0.5 M NaCl; 5 mM imidazole; 8 M urea; pH 7.4). Following centrifugation at 13,400 x g for 20 min at 4˚C, the supernatant containing the dissolved inclusion bodies was collected. This supernatant was then combined with Ni-NTA and incubated for 1 h at 4˚C. Similarly, the supernatant from the expression of the fusion protein was also combined with Ni-NTA and incubated for 1 h at 4˚C. The inclusion bodies in the precipitate were dissolved in binding buffer (20 mM sodium phosphate; 0.5 M NaCl; 5 mM imidazole; 8 M urea; pH 7.4). Following centrifugation at 13,400 x g for 20 min at 4˚C, the supernatant containing the dissolved inclusion bodies was collected. This supernatant was then combined with Ni-NTA and incubated for 1 h at 4˚C. Similarly, the supernatant from the expression of the fusion protein was also combined with Ni-NTA and incubated for 1 h at 4˚C. The inclusion body-expressed protein underwent gradient renaturation in refolding buffer (20 mM sodium phosphate; 0.5 M NaCl; 6-0 M urea gradient; pH 7.4). The purified protein was concentrated using an ultrafiltration tube, and the concentration of the purified fusion protein was determined using a BCA assay kit. Subsequently, the complete amino acid sequences of hTSHR410, hTSHR290 and hTSHR289 were imported into ExpaSy-ProtParam software (https://web.expasy.org/protparam/), and various physical and chemical parameters, including the molecular weight, of the protein were calculated through the software analysis, and the molecular weight of each fusion protein was estimated. The predicted molecular weights of hTSHR289, hTSHR410 and hTSHR290 are ~47, 70 and 39 kDa respectively.

Western blot analysis. SDS-PAGE and western blot analysis were used to characterize the three hTSHR fusion proteins purified in the previous step. Proteins were extracted using the ultrasonic disruption method (power 200 w; ultrasound was on for 2 sec and off for 3 sec), and SDS-PAGE loading buffer (cat. no. P1040, Beijing Solarbio Science & Technology Co., Ltd.) was added to the extracted proteins, which were boiled for 5-10 min. The concentration of the protein was detected using a BCA protein quantification kit. Each lane was loaded with 5 μg of protein. Prepared samples (purified hTSHR fusion protein with protein extraction buffer) were loaded into the sample wells of the SDS-PAGE gel (10%) and electrophoresed at 120 V. The SDS-PAGE gel was stained with Coomassie Brilliant Blue (Beijing Solarbio Science & Technology Co., Ltd.), or the proteins in the SDS-PAGE gel were electro-transferred to a PVDF membrane (Beijing Solarbio Science & Technology Co., Ltd.). The membrane was blocked with 5% non-fat powdered milk (cat. no. D8340; Beijing Solarbio Science & Technology Co., Ltd.) at room temperature for 2 h. The PVDF membrane was then blocked and incubated with antibodies, including TSHR 3B12 (1:1,000; sc-53542; Santa Cruz Biotechnology, Inc.; 4˚C; 12 h) and His (1:1,000; 1B7G5; Proteintech Group, Inc.; 4˚C; 12 h). The next day, following incubation with secondary antibodies [Goat Anti-Mouse IgG H&L (HRP); 1:10,000; ab205719; Abcam] for 2 h at room temperature, visualization was carried out using ECL reagent (Beijing Solarbio Science & Technology Co., Ltd.) on an automated chemiluminescence imager.

Direct ELISA using hTSHR fusion protein as the antigen (hTSHR ELISA) and specificity. The three fusion proteins were coated as antigens on the plate of enzymes. Following repeated experiments, it was determined that coating with 1 μg/well of antigen at 4˚C overnight and blocking with 200 μl 1% BSA (Jiangsu Aidisheng Biotechnology Co., Ltd.) per well at 37˚C for 2 h were the optimal conditions. Different serum samples were diluted in a gradient of 1:1,000 (optimized dilution ratio) and used as the primary antibody, with 100 μl diluted serum added per well. Duplicate test wells and control wells were set up and then incubated at 37˚C for 2 h. Following the addition of 100 μl HRP-labeled antibody (1:10,000; cat. no. D110150; Sangon Biotech Co., Ltd.), the plate was incubated at 37˚C for a further 2 h, followed by color development with tetramethyl-benzidine substrate for 15 min at 37˚C. The absorbance value at 450 nm was then determined using an ELISA reader.

Animal study. A total of 48 female BALB/c mice aged 5-6 weeks and weighing 20±2 g were obtained from Jiangsu Cavens Experimental Animals Co., Ltd. The mice were housed under specific pathogen-free conditions at the Experimental Animal Research Platform of The Second Hospital of Lanzhou University. The mice were raised in a specific pathogen-free environment, the temperature was 18-22˚C and the humidity was 50-60%, with a 12/12-h light/dark cycle. The feed was purchased from Beijing Keao Xieli Feed Co., Ltd. (cat. no. 1016706714625204224). The drinking water came from the experimental animal research platform. Both the feed and water underwent high-temperature and high-pressure sterilization treatment. Mice had *ad libitum* access to food and water. Food, water, air, bedding and all other supplies entering the animal center barrier system were sterilized with high temperature and high pressure, and were sterilized by irradiation through the transfer window before entering and exiting the animal research platform. The mice were randomly divided into 4 groups, with 12 mice in each group, which were the hTSHR410 fusion protein immune mouse group, hTSHR289 fusion protein immune mouse

group, hTSHR290 fusion protein immune mouse group and normal saline control group. The animal experiments received approval from the Animal Welfare and Ethics Committee of The Second Hospital of Lanzhou University (approval no. D2023-156; Lanzhou, China). After reviewing the literature and combining the test results of previous studies, mice were immunized with a 1:1 mixture of fusion protein injected at 4 points on the back of the mice with complete Freund's adjuvant (the first injection) and incomplete Freund's adjuvant (the second two injections) (20,21). Each female BALB/c mouse was injected subcutaneously with 50 μg hTSHR fusion protein at 4 points on the back, and the control group was injected with normal saline. Three immunizations were given at weeks 0, 3 and 6. Mice were anesthetized by intraperitoneal injection of sodium pentobarbital (50 mg/kg) and euthanized by anesthesia overdose (intraperitoneal injection of sodium pentobarbital; 100 mg/kg). The Animal Research: Reporting of *In Vivo* Experiments guidelines were followed (22).

Mouse serum analysis. Blood was collected via cardiac puncture 2 weeks after the completion of immunization under deep anesthesia (30 mg/kg sodium pentobarbital; intraperitoneal injection). The extracted blood was placed in 1.5-ml Eppendorf tubes and left to stand at room temperature. Next, a centrifuge was set to 3,000 x g and samples were centrifuged for 15 min at room temperature to separate the serum, which was then stored at -20˚C. The present study utilized the thyroxine (T4) ELISA kit (cat. no. JL10849; Shanghai Jonlnbio Industrial Co., Ltd.), the TSH ELISA kit (cat. no. JM-11776M1; Jingmei Biotechnology Co., Ltd.) and the TRAb ELISA kit (cat. no. ZY-TRAb-MU; Zeye Biotechnology Co., Ltd.) to assess the levels of TSH, T4 and TRAb in the serum of each group of mice. A total of 10 μl of serum was extracted from each mouse in each group. The serum was diluted by 1:4 using the sample dilution solution in the aforementioned kits, and then the analysis was carried out according to the manufacturer's instructions. Readings were obtained at 450 nm using an ELISA reader. The procedure was repeated three times for each assessment.

Histological analysis. Mice were euthanized using an overdose anesthetic method (intraperitoneal injection of sodium pentobarbital; 100 mg/kg), and the thyroid glands were dissected. The thyroid tissue was soaked in 4% paraformaldehyde for >48 h at room temperature. After fixation, the tissues were dehydrated, sequentially soaked in 75% alcohol, 95% alcohol and absolute ethanol for gradient dehydration, sequentially soaked in two xylenes (Tianjin Fuyu Fine Chemical Co., Ltd.) and paraffin-embedded, and were then sectioned using a Leica microtome (thickness, 5 μm; Leica Microsystems, Inc.). Subsequently, the slices were placed in a baking machine and baked at 75˚C for 1 h. After deparaffinization, hematoxylin was added dropwise to the slices and these were incubated at room temperature for 5 min. Differentiation was performed by adding hydrochloric acid ethanol dropwise to the slices and incubating at room temperature for 3-5 sec. Finally, eosin solution was added dropwise to the slices and the slices were incubated at room temperature for 1-2 min. After the neutral gum was completely dried, observations and scans were performed using a light microscope.

Flow cytometry of T cell subsets. Following euthanasia, splenic tissues were retrieved from the immunized mice and placed in 1640 culture medium (Gibco; Thermo Fisher Scientific, Inc.). The spleen tissues were dissected into small pieces using a surgical blade. Subsequently, the spleen tissue was ground on a 100-mesh cell strainer to obtain a single-cell suspension. Following centrifugation at 350 x g at 4˚C for 10 min, cells were collected, treated with red blood cell lysis buffer at room temperature for 10 min, washed with PBS and then centrifuged at 350 x g at 4˚C for 10 min to obtain lymphocytes. Lymphocytes ($2x10^6$ cells) were stained using allophycocyanin (APC)/phycoerythrin (PE)/FITC markers. Cells were analyzed using the CytoFLEX LX Flow Cytometer (Beckman Coulter, Inc.). Reported results were analyzed using the CytExpert software (version 2.5; Beckman Coulter, Inc.) of the CytoFLEX LX flow cytometer to characterize T cell subsets. The analyte detectors were as follows: $CD3^+$ antibody (cat. no. 565643; Becton, Dickinson and Company), $CD4^+$ antibody (cat. no. F21004A02; Multi Sciences Biotech), $CD8^+$ antibody (cat. no. F2100801; Multi Sciences Biotech), CD25 antibody (cat. no. E-AB-F1102C; Wuhan Elabscience Biotechnology Co., Ltd.) and CD122 antibody (cat. no. E-AB-F1029D; Wuhan Elabscience Biotechnology Co., Ltd.). The analyte reporters were as follows: $CD3^+$, APC; $CD4^+$, PE; $CD8^+$, FITC; CD25, FITC; and CD122, PE.

Statistical analysis. Statistical analysis was performed using GraphPad Prism 8.0 software (Dotmatics) and SPSS 26.0 software (IBM Corp.). Quantitative data with normal distribution are presented as the mean ± standard deviation, while data with a skewed distribution are presented as the median (quartile), and count data are presented as absolute values or percentages. One-way ANOVA with Tukey's post hoc test was used for comparisons of multiple groups of parametric data. Categorical variables were compared using χ^2 tests to compare all groups and Bonferroni correction was applied to the P-values. The Kruskal-Wallis test with Dunn's post hoc test was used for non-parametric data. $P<0.05$ was considered to indicate a statistically significant difference. All experiments were repeated in triplicate.

Results

Different fusion proteins of hTSHR. According to the full-length receptor gene sequence of human TSHR, different hTSHR protein sequences were extracted: hTSHR410, hTSHR289 and hTSHR290 (amino acid sequences shown in Fig. 1A). The recombinant plasmid was obtained by ligating the gene sequences corresponding to the aforementioned hTSHR amino acid sequences with the vector. The results of agarose gel electrophoresis after PCR amplification are shown in Fig. 1B. Recombinant plasmids with correctly framed reading sequences were selected for expression in *Escherichia coli*, followed by induction with IPTG, purification and visualization on SDS-PAGE gels, where three distinct bands were observed (Fig. 1C-E). Based on SDS-PAGE, the molecular weight of the single band in Fig. 1C was estimated to be ~47 kDa, that of the single band in Fig. 1D was ~70 kDa and that of the single band in Fig. 1E was ~39 kDa. These results indicated that the purified proteins had molecular

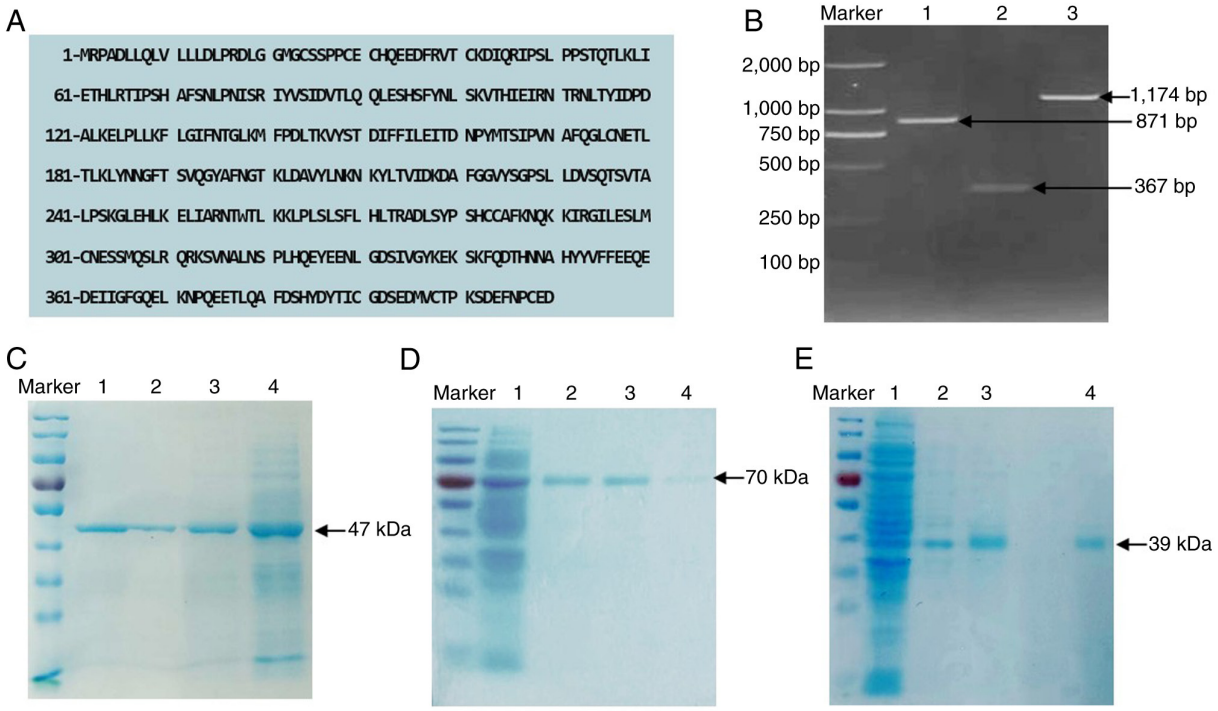

Figure 1. Expression of different fusion proteins of hTSHR. (A) Sequence of different fusion proteins of hTSHR. hTSHR410 (amino acid sequence 21-410), hTSHR289 (amino acid sequence 1-289) and hTSHR290 (amino acid sequence 290-410). (B) Restriction fragments on an agarose gel. Lane 1 shows hTSHR289, lane 2 shows hTSHR290 and lane 3 shows hTSHR410. (C) SDS-PAGE of purified hTSHR289. Lanes 1-3 show different imidazole-purified proteins (250, 350 and 150 mmol/ml, respectively) and lane 4 is unpurified fusion protein after fragmentation. (D) hTSHR410 fusion protein. Lane 1 is the unpurified fusion protein after fragmentation and lanes 2-4 show different imidazole-purified proteins (150, 250 and 350 mmol/ml, respectively). (E) hTSHR290 fusion protein. Lane 1 is the unpurified fusion protein after fragmentation and lanes 2-4 show different imidazole-purified proteins (150, 250 and 350 mmol/ml, respectively). hTSHR, human thyroid-stimulating hormone receptor.

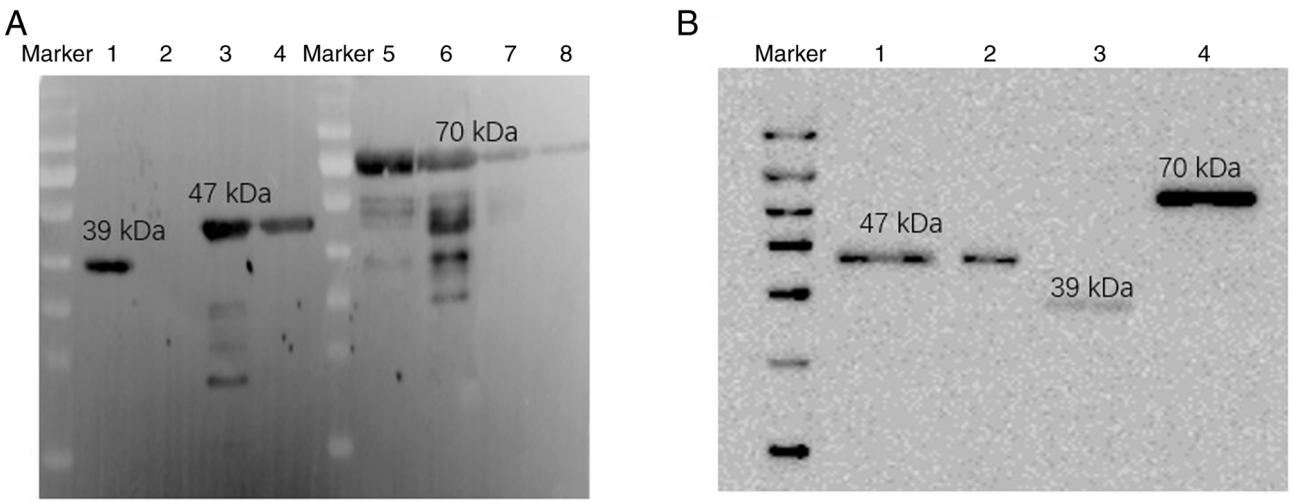

Figure 2. Binding of different fusion proteins with TSHR antibodies and His antibodies. (A) Binding with TSHR antibodies. hTSHR290 shows bands at 39 kDa (lane 1); blank (lane 2) hTSHR289 shows bands at 47 kDa (lanes 3 and 4); hTSHR410 shows bands at 70 kDa (lanes 5-8). (B) Binding with His antibodies. hTSHR289 shows bands at 47 kDa (lanes 1 and 2); hTSHR290 shows bands at 39 kDa (lane 3); hTSHR410 shows bands at 70 kDa (lane 4). His, histidine; hTSHR, human thyroid-stimulating hormone receptor.

weights consistent with the expected values, indicating that they were hTSHR fusion proteins.

hTSHR fusion protein validation. Fusion proteins were expressed in the prokaryotic system and single bands were obtained by SDS-PAGE after purification. In order to accurately identify the three different hTSHR fusion proteins, validation using western blotting was performed. TSHR monoclonal antibody (3B12), His antibody and the three different fusion proteins (hTSHR410, hTSHR289 and hTSHR290) were assessed using western blotting. The results showed clear protein bands at 70, 47 and 39 kDa (Fig. 2A and B). This demonstrated that the purified fusion proteins were hTSHR fusion proteins.

Binding activity of different hTSHR fusion proteins to an IgG antibody verified using an ELISA. In order to establish a convenient and stable method for distinguishing the types of TRAb and to validate the biological activity of the different hTSHR fusion proteins obtained, the age, sex, and FT3, FT4, TSH and TRAb levels were analyzed in five groups of recruited patients. There were no statistically significant differences in the age or sex among the patients in each group. This is summarized in Table II.

In the present study, an ELISA was carried out to assess the binding activity of serum IgG antibodies to hTSHR410, hTSHR289 and hTSHR290 fusion proteins in serum samples from the aforementioned five groups: Hyperthyroidism ($TRAb^+$ and $TRAb^-$), hypothyroidism ($TRAb^+$ and $TRAb^-$) and healthy individuals. The results revealed that the absorbance [optical density (OD)450 nm] of hTSHR289 fusion protein with serum from patients in the hyperthyroidism $TRAb^+$, hyperthyroidism $TRAb^-$, hypothyroidism $TRAb^-$ and hypothyroidism $TRAb^+$ groups was increased compared with that in healthy individuals ($P<0.05$). Among these, the serum from patients with hyperthyroidism $TRAb^+$ showed the highest binding OD450 value with hTSHR289 fusion protein. Similarly, the binding OD450 values of hTSHR290 fusion protein with serum from patients in the hyperthyroidism $TRAb^-$, hypothyroidism $TRAb^+$, hypothyroidism $TRAb^-$ and hypothyroidism $TRAb^-$ groups were all higher compared with those in healthy individuals ($P<0.05$). Among these, the serum from patients with hypothyroidism $TRAb^+$ exhibited the highest binding OD450 value with the hTSHR290 fusion protein. Furthermore, the binding OD450 values of the hTSHR410 fusion protein with serum from patients in the hyperthyroidism $TRAb^+$, hyperthyroidism $TRAb^-$, hypothyroidism $TRAb^+$ and hypothyroidism $TRAb^-$ groups were all higher compared with those in healthy individuals ($P<0.05$; Fig. 3).

Based on Figs. 2 and 3, both the hTSHR290 and hTSHR289 fusion proteins were revealed to exhibit biological activity and strong antigenicity. Thus, they could be used as antigens to establish corresponding serological detection methods for the determination of TSAb and TBAb.

Changes in thyroid function of immunized mice. An ELISA was carried out to detect the binding activity of the three fusion proteins with serum from patients with hyperthyroidism and hypothyroidism, demonstrating the biological activity of the prepared fusion proteins. In order to further validate the immunogenicity of the different fusion proteins, BALB/c mice were immunized with the fusion proteins.

T4, TSH and TRAb may be effective indicators for evaluating thyroid function. Following the immunization of mice, serum samples from the four groups of mice were tested using T4, TSH and TRAb ELISA kits. Analysis revealed that the T4 levels in mice immunized with hTSHR289 (aa1-289) fusion protein were 74.06±8.55 ng/ml, and were significantly higher than those in the control group (60.01±7.74 ng/ml) and exceeded the normal range for T4 levels (52.27-67.75 ng/ml). The T4 levels in mice immunized with hTSHR410 (aa21-410) were 66.17±5.48 ng/ml, and were higher compared with those in the control group (60.01±7.74 ng/ml). The T4 levels in mice immunized with hTSHR290 (aa290-410) were 44.85±9.70 ng/ml, and were lower compared with those in the

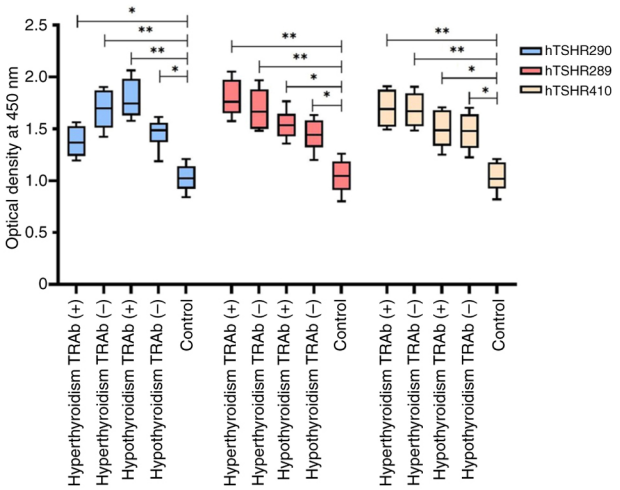

Figure 3. Specific binding of different fusion proteins as antigens with antibodies. Binding of fusion proteins from the hTSHR290, hTSHR289 and hTSHR410 groups with sera from different groups of patients. $^*P<0.05$, $^{**}P<0.01$. One-way ANOVA with Tukey's post hoc test was used for comparisons of multiple groups of parametric data. hTSHR, human thyroid-stimulating hormone receptor; TRAb, thyroid-stimulating hormone receptor antibodies.

control group (60.01±7.74 ng/ml), and these differences were statistically significant ($P<0.05$) (Fig. 4A).

The TSH levels in mice in the hTSHR290 (30.13±1.27 pg/ml) group were significantly higher and the TSH levels in the hTSHR289 (28.34±0.90 pg/ml) group was significantly higher than those in the control group (28.82±0.55 pg/ml), exhibiting a statistically significant difference ($P<0.05$). The TSH levels in mice in the hTSHR410 group (28.79±0.81 pg/ml) did not differ significantly from those in mice in the control group (Fig. 4C).

The TRAb levels in mice immunized with hTSHR289 (13.51±2.26 ng/ml), hTSHR410 (12.47±3.48 ng/ml) and hTSHR290 (13.05±2.53 ng/ml) were all increased compared with those in the control group (4.16±1.36 ng/ml), which was statistically significant ($P<0.05$), as shown in Fig. 4B.

Following the determination of thyroid function indicators, including T4, TSH and TRAb, to further ascertain alterations in thyroid function in immunized mice, H&E staining was conducted on the thyroid tissues and various pathological changes were observed. Thyroid tissues from 7/12 of the hTSHR289 mice exhibited diffuse hyperplasia with increased cellularity. Epithelial proliferation led to the formation of papillary projections into the follicular lumen. The colloid within the follicular lumen was sparse, exhibiting scalloped edges, along with varying sizes of absorption vacuoles. The epithelium consisted of tall columnar cells with basal nuclei that were crowded, round or elliptical and irregular in shape, indicative of pathological changes in the thyroids of hyperthyroid mice (Fig. 5A and B). In the thyroid tissues of 8/12 of the hTSHR290 mice, the thyroid follicular epithelium was composed of tall columnar cells with loosely arranged basal nuclei, exhibiting round or elliptical nuclei that were irregular in shape. Some follicles exhibited destruction and atrophy, accompanied by extruded colloid, representing pathological changes in hypothyroid mouse thyroids (Fig. 5C and D). The thyroid lesions in 7/12 of the hTSHR410 mice manifested as

Table II. Clinical characteristics of all subjects.

Variable	Hyperthyroidism ($TRAb^+$)	Hyperthyroidism ($TRAb^-$)	Hypothyroidism ($TRAb^+$)	Hypothyroidism ($TRAb^-$)	Control	P-value
Age, years	33.91±13.06	35.10±13.76	33.17±18.97	37.4±16.86	34.9±12.23	0.631[a], 0.346[b], 0.593[c], 0.275[d]
Sex, n						
Male	10	9	11	10	12	0.592[a], 0.417[b], 0.791[c], 0.592[d]
Female	20	21	19	20	18	
FT3, pmol/l (normal range, 2.77-6.31 pmol/l)	15.19±9.23	13.67±4.80	2.29±1.71	1.87±0.99	4.13±1.35	0.012[ae] 0.030[be], 0.021[ce], 0.008[de]
FT4, pmol/l (normal range, 10.44-24.38 pmol/l)	41.99±16.21	38.28±14.32	4.12±3.48	3.85±2.52	16.61±3.50	0.035[ae], 0.026[be], 0.012[ce], 0.007[de]
TSH, μIU/ml (normal range, 0.38-4.34 μIU/ml)	0.10 (0.10, 0.30)	0.08 (0.06,0.40)	68.09 (33.70,108.76)	73.77 (41.43,116.29)	2.64 (1.80,3.41)	0.006[ae], 0.007[be], 0.036[ce], 0.023[de]
TRAb, IU/l (normal range, 0.00-60.00 U/ml)	20.00 (11.00, 30.00)	0.77 (0.36,1.15)	16.64 (7.39, 30.00)	0.54 (0.43, 0.61)	0.38 (0.14, 1.07)	0.008[ae], 0.558[b], 0.021[ce], 0.642[d]
TG, ng/ml (normal range, 1.00-39.00 ng/ml)	601.56 (28.00, 1300.00)	548.50 (30.60, 1300.00)	572.04 (16.30, 1300.00)	483.41 (21.00, 1300.00)	15.70 (3.28, 35.40)	0.016[ae], 0.017[be], 0.009[ce], 0.006[de]
TPOAb, U/ml (normal range, 0.0-1.5 IU/l)	54.37 (0.50, 314.10)	61.43 (0.20, 368.00)	92.25 (2.00, 600.00)	85.82 (0.63, 438.50)	0.53 (0.00, 1.08)	0.023[ae], 0.037[be], 0.018[ce], 0.025[de]

[a]Hyperthyroidism ($TRAb^+$) group vs. healthy controls; [b]hyperthyroidism ($TRAb^-$) group vs. healthy controls; [c]hypothyroidism ($TRAb^+$) group vs. healthy controls; [d]hypothyroidism ($TRAb^-$) group vs. healthy controls; [e]$P<0.05$. One-way ANOVA was used for the comparison of multiple groups of data (age, FT3 and FT4), The categorical variables were compared using χ^2 tests to compare all groups and Bonferroni correction was applied to the P-values (sex), Kruskal-Wallis test was used for non-parametric data (TSH, TRAb, TG and TPOAb). Tukey's (age, FT3, FT4 and Dunn's (TSH, TRAb, TG and TPOAb) post hoc tests were used for multiple comparisons. FT3, free triiodothyronine; FT4, free thyroxine; TSH, thyroid-stimulating hormone; TRAb, thyroid-stimulating hormone receptor antibodies; TG, thyroglobulin; TPOAb, thyroid peroxidase antibodies.

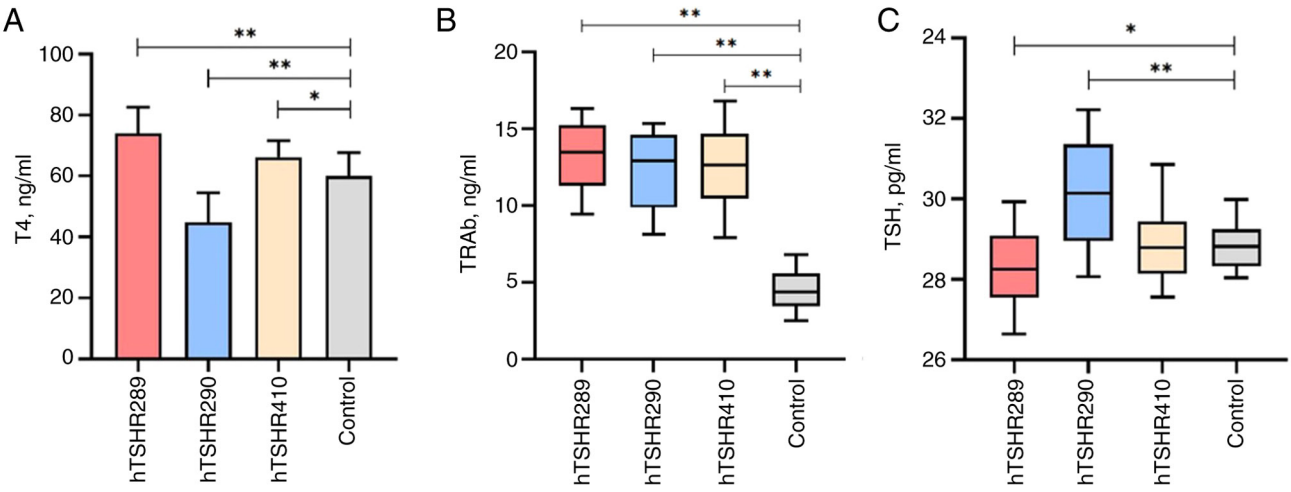

Figure 4. Changes in mouse thyroid function. Measurements of post-immunization levels of (A) T4, (B) TRAb and (C) TSH in mice. *P<0.05, **P<0.01. One-way ANOVA with Tukey's post hoc test was used for comparisons of multiple groups of parametric data. hTSHR, human thyroid-stimulating hormone receptor; T4, thyroxine; TRAb, thyroid-stimulating hormone receptor antibodies; TSH, thyroid-stimulating hormone.

focal distribution, with some follicles displaying destruction, atrophy and extruded colloid. Regeneration of some follicular epithelium and increased fibrous tissue between the follicles were observed (Fig. 5E and F). The thyroid tissue of mice in the control group revealed that the follicular structure of the thyroid gland was normal, the follicle was round or oval, the epithelial cells were arranged in a single flat shape, and the follicle was filled with glia (Fig. 5G and H). No animals were prematurely euthanized in the present study, and all animals completed the predetermined protocol. The results reflected the respective mean values of all measurements for all randomized animals.

$CD4^+$ T cells and $CD8^+$ T cells participate in immune responses in mice. The predominant causes of thyroid cell damage and TSHR antibody production in AITD include the activation of $CD4^+$ T cells. Simultaneously, cytokines produced following the activation of $CD4^+$ T cells stimulate $CD8^+$ T cells to destroy thyroid cells, particularly thyroid cells in patients with HT (23,24). Therefore, the overall balance, proliferation and activation of $CD4^+$ T cells and $CD8^+$ T cells are of importance in the pathogenesis of AITD.

In the present study, the immune response was further investigated following the immunization of mice with three types of hTSHR fusion proteins as antigens. Flow cytometry was utilized to determine the proportions of $CD4^+$ and $CD8^+$ T cells in splenocytes of each group of mice. The proportion of $CD4^+$ T cells in the three immunization groups was increased compared with that in the control group, and the difference was statistically significant. The proportion of $CD8^+$ T cells in the three immunization groups was increased compared with that in the control group; however, the difference was not statistically significant (Fig. 6).

$CD4^+CD25^+$ T cells and $CD8^+CD122^+$ T cells participate in the immune response in mice. $CD4^+CD25^+$ T cells and $CD8^+CD122^+$ T cells are associated with the occurrence and severity of AITD (25,26). Flow cytometry was carried out to detect the numbers of $CD4^+CD25^+$ T cells and $CD8^+CD122^+$ T cells in spleen cells from each group of mice. Analysis revealed that the numbers of $CD4^+CD25^+$ T cells and $CD8^+CD122^+$ T cells in spleen cells of the hTSHR289, hTSHR290 and hTSHR410 groups were decreased compared with those in the control group (Fig. 7).

Discussion

The occurrence of AITD affects hundreds of millions of individuals worldwide, with the main types being GD and HT, characterized by hyperthyroidism and hypothyroidism, respectively (27). GD is a diffuse goiter and hyperthyroidism condition associated with the presence of TSHR and its autoantibodies (28). TSHR contains three structural domains: The LRRD, hinge region and TMD (29-31). The full-length TSHR can be proteolytically cleaved into an A subunit (aa1-289) and a transmembrane B subunit (aa370-764) (32,33). The A subunit can be shed from the full-length TSHR, becoming an inducer of TRAb autoantibodies (34). Studies have shown that TSAb, TSH and TBAb can bind to the leucine-rich repeat region, and some TBAb and neutral antibodies can also bind to linear epitopes in other structural domains of TSHR (35-37). Furthermore, the epitopes recognized by TSH, TSAb and TBAb on TSHR are spatially close and exhibit some overlap (36,37). Therefore, based on the structural characteristics of TSHR and its binding properties with autoantibodies, active hTSHR fusion proteins were produced that mimic the natural protein structure and function of hTSHR. These include the hTSHR289 fusion protein containing the active LRRD of hTSHR (TSHR A subunit), the hTSHR410 (aa1-410) fusion protein containing the entire ECD of TSHR, and the hTSHR290 fusion protein containing the carboxyl-terminal region of the ECD including the hinge region of TSHR (TSHR aa290-410).

The present study further investigated the immunogenicity and clinical significance of different fusion proteins of TSHR using serological and *in vivo* experiments. In a study by Zulkarnain *et al* (38), the authors used a prepared fusion protein of the TSHR169 fragment to bind with the sera of 20 patients with GD, exploring methods for the diagnosis of GD. In the

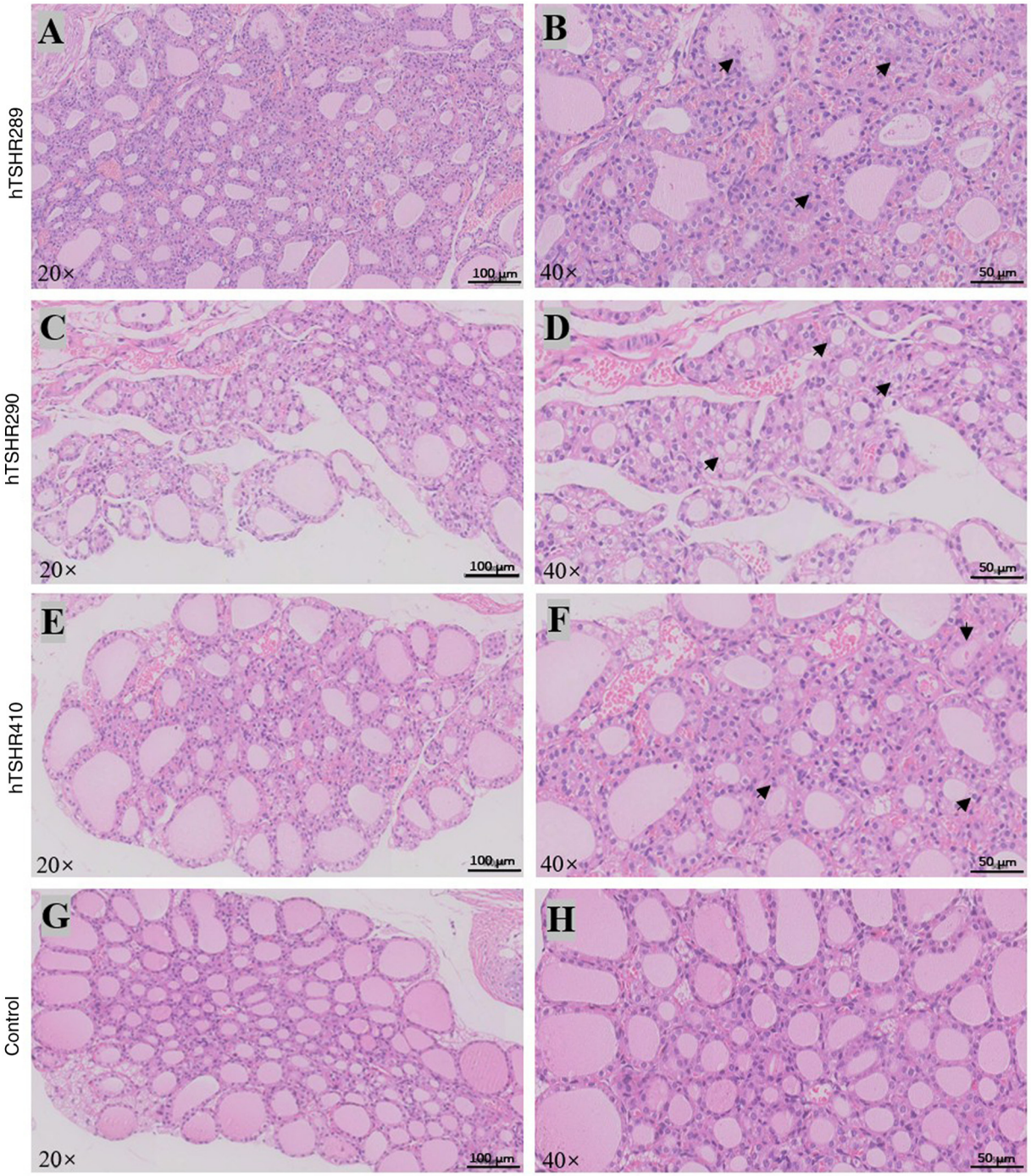

Figure 5. Pathological changes in mouse thyroid tissues. Representative images of pathological changes in the thyroid glands of mice from the hTSHR289 group after immunization following H&E staining at a magnification of (A) x20 and (B) x40. Arrows indicate diffuse hyperplasia with an increase in follicular epithelial cells and papillary protrusions Schematic representation of pathological changes in the thyroid glands of mice from the hTSHR290 group after immunization following H&E staining at a magnification of (C) x20 and (D) x40. Arrows indicate high columnar cells with destroyed and atrophied follicles accompanies by extruded colloids. Schematic representation of pathological changes in the thyroid glands of mice from the hTSHR410 group after immunization following H&E staining at a magnification of (E) x20 and (F) x40. Arrows indicate high columnar cells, follicular epithelial cell proliferation and fibrous tissue increase. Schematic representation of pathological changes in the thyroid glands of mice from the control group after immunization following H&E staining at a magnification of (G) x20 and (H) x40. hTSHR, human thyroid-stimulating hormone receptor.

present study, serum-based validation was conducted using the ELISA method. Strong specific binding reactions were observed between the hTSHR289 fusion protein and the sera of patients with clinically diagnosed hyperthyroidism with $TRAb^+$. The sera of patients diagnosed with hyperthyroidism $TRAb^+$ primarily contain TSAb, indicating that TSAb largely binds specifically to the TSHRA subunit (4). The hTSHR290 fusion protein exhibited the strongest binding reaction with the sera of patients with hypothyroidism who were $TRAb^+$, and even the sera of patients clinically diagnosed with hypothyroidism who were $TRAb^-$ displayed a binding reaction with the hTSHR290 fusion protein. Furthermore, the results of the present study indicated that the carboxyl-terminal end of TSHR (aa290-410) may be an antigenic determinant for recognizing TBAb.

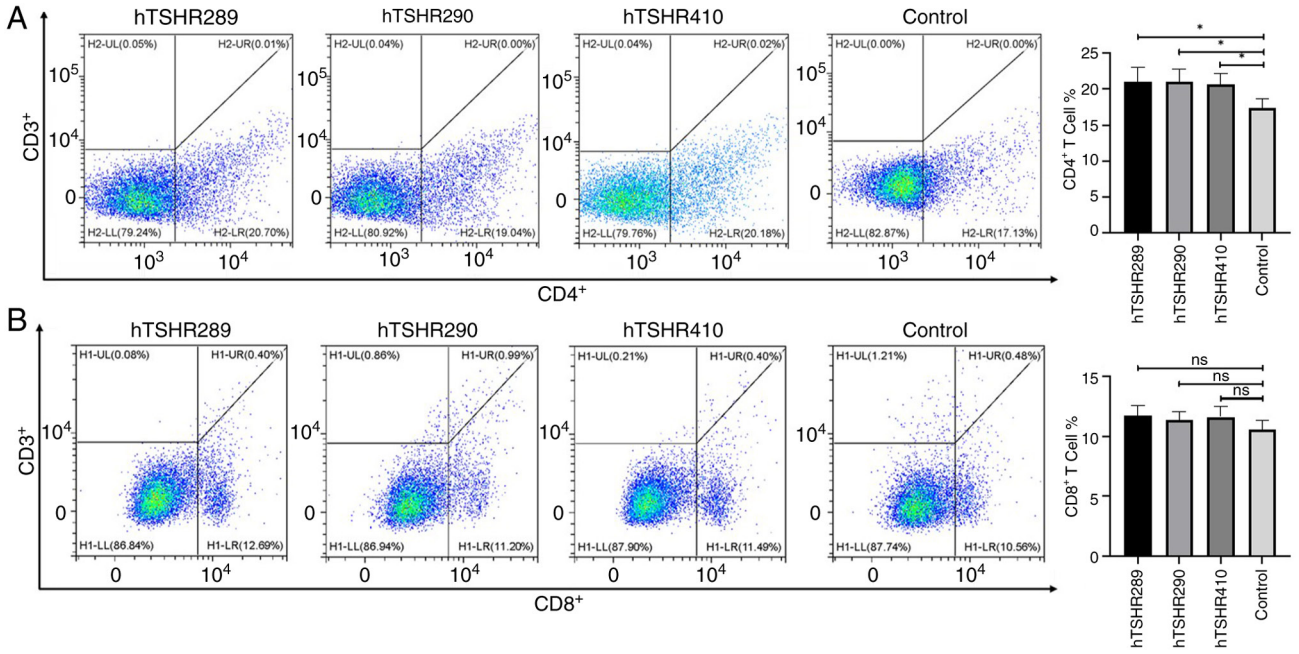

Figure 6. Changes in T cell subsets in mice after immunization. (A) Flow cytometry analysis of changes in $CD4^+$ T cells in the hTSHR289, hTSHR290 and hTSHR410 groups after immunization. (B) Flow cytometry analysis of changes in $CD8^+$ T cells in the hTSHR289, hTSHR290 and hTSHR410 groups after immunization. *P<0.05 (One-way ANOVA with Tukey's post hoc test). hTSHR, human thyroid-stimulating hormone receptor; ns, not significant.

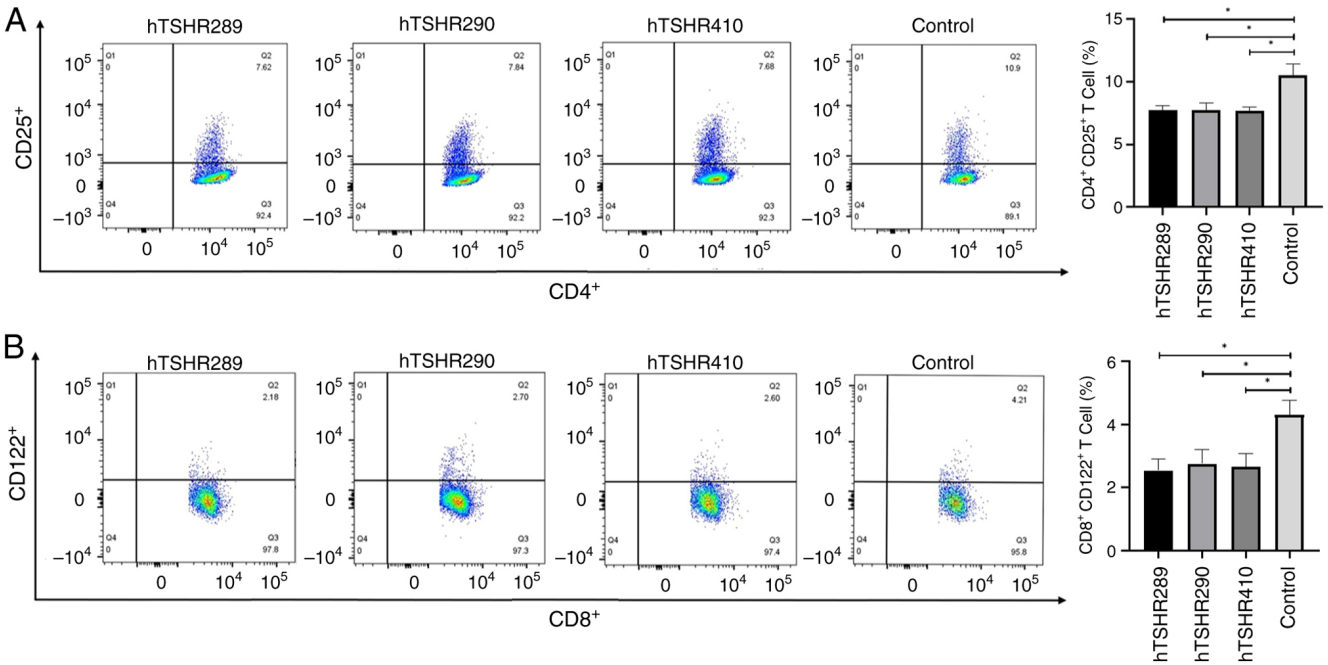

Figure 7. Changes of specific regulatory T cell subsets in mice after immunization. (A) Flow cytometry analysis of changes in $CD4^+CD25^+$ T cells in the hTSHR289, hTSHR290 and hTSHR410 groups after immunization. (B) Flow cytometry analysis of changes in $CD8^+CD122^+$ T cells in the hTSHR289, hTSHR290 and hTSHR410 groups after immunization. *P<0.05 (One-way ANOVA with Tukey's post hoc test. hTSHR, human thyroid-stimulating hormone receptor.

In previous years, numerous studies have used eukaryotic or adenoviral vectors or plasmids as the basis for investigating the role of TSHR. Researchers have expressed concerns that prokaryotically prepared TSHR proteins may lack immunogenicity, which was also a focus of the present study. For studies of TSHR-induced thyroid disease models, current research often employs adenoviral vectors carrying the TSHR A subunit or plasmid-induced GD models. This method requires technical skills and specialized equipment support, and is expensive (16,39-41). The present study prepared different fusion proteins of TSHR in a prokaryotic system, which is simple to operate, has high production yields (higher than eukaryotic systems) (42) and is cost-effective. Subcutaneous injection of fusion proteins to establish disease models has been

utilized in various disease models and has been demonstrated to be effective (20,21). Previous investigations have noted that immunization of BALB/c mice with the ECD protein of human thyroid-stimulating hormone receptor induced thyrotropin-binding inhibitory immunoglobulins (TBII) in the serum, subsequently leading to thyroid pathology (11,39,43). In addition, a study has demonstrated that repetitive intravenous injections of 0.1 mg/kg of cyclic peptide 19, a derivative of the first cytoplasmic loop of TSHR rich in LRRDs, could reduce thyroid hyperplasia in a long-term mouse model of GD. This intervention also led to elevated T4 levels and a reduction in sinus tachycardia (11). Therefore, the important role of LRRDs needs to be carefully considered. In the present study, three fusion proteins with different biological activities were identified through patient serum analysis. To gain a deeper understanding of the role of TSHR as a primary antigen in the pathogenesis of AITD, a series of experiments were conducted using BALB/c mice to investigate the immunogenicity and clinical significance of TSHR fusion proteins.

In the present investigation, using various fusion proteins of hTSHR as immunogens, immune responses were induced in mice that mimicked those triggered by native hTSHR protein antigens. Analysis revealed that mice immunized with the hTSHR289 fusion protein exhibited significantly elevated levels of TSHR antibodies and T4 compared with the control group. Histopathological examination of thyroid tissue sections revealed pathological changes consistent with hyperthyroidism. These findings underscore the potential utility of hTSHR fusion proteins in developing experimental models of thyroid disorders. Compared with the control group, the hTSHR290 group of mice exhibited a significant decrease in T4 levels, along with increased levels of TRAb and TSH. Pathological examination of thyroid tissue sections revealed pathological changes consistent with hypothyroidism, such as the presence of tall columnar cells comprising the thyroid follicular epithelium with nuclei located basally, partial follicle destruction and atrophy, as well as extracellular colloid leakage. When comparing the hTSHR410 group with the control group, significant increases in TRAb and T4 levels were observed, while TSH values did not significantly differ between the groups. The pathological presentation of thyroid tissue indicated focal distribution of fibrotic changes. Collectively, the fusion protein hTSHR289 (TSHRA subunit; aa1-289) induced primarily stimulatory antibodies in mice, leading to the development of GD. The fusion protein hTSHR290 (carboxyl-terminal region of TSHR; aa290-410) acted as an immunogenic antigen, resulting in the production of TBAb, and thus, inducing hypothyroidism in mice. hTSHR410 fusion protein (entire ECD of TSHR) triggered a cross-reactive immune response in mice, among which the pathological changes associated with GD were more prominent. However, as a single model for research into AITD, the hTSHR410 fusion protein as an immunogen may not be an ideal choice. Therefore, the utilization of hTSHR289 and hTSHR290 fusion proteins as immunogens to induce hyperthyroidism and hypothyroidism animal models, respectively, would be beneficial for in-depth exploration of the occurrence, progression and treatment of AITD. Furthermore, inducing disease occurrence through fusion proteins is close to the natural process of autoimmune disease development. The animal models induced and constructed in the present study will be more conducive to the research of AITD.

The activation of $CD4^+$ T cells serves as the primary mechanism in AITDs leading to thyroid cell damage and the production of TRAb (31,44). In HT, thyroid cells are destructed by inflammatory infiltration composed of $CD8^+$ T cells, $CD4^+$ T cells, macrophages and plasma cells (24). Both $CD4^+$ and $CD8^+$ T cells infiltrate the thyroid gland in varying proportions, resulting in altered thyroid function and the onset of HT and GD. Furthermore, they are closely associated with TRAb levels, serving a key role in predicting treatment outcomes (44,45). The animal experiments in the present study indicated that the hTSHR fusion protein induced alterations in mice, leading to hyperthyroidism, hypothyroidism and inflammatory responses. Further confirming the immunogenicity of hTSHR fusion proteins and their role in inducing pathogenic TRAb in mice, the present results indicated that the ratio of $CD4^+$ T cells and $CD8^+$ T cells was altered in immunized mice.

The specific expression of CD25 on the surface of $CD4^+$ T cells accounts for ~10% of peripheral blood $CD4^+$ T cells. Inhibiting abnormal or excessive immune responses against self, microbial and environmental antigens is associated with a wide range of autoimmune diseases (autoimmune gastritis, thyroiditis and type 1 diabetes) (46). Deficiency of $CD4^+CD25^+$ T cells leads to various autoimmune and inflammatory states in mice (47). Studies have found that the frequency of $CD4^+CD25^+$ T cells in lupus-prone mice was lower than that in normal mice (48,49). A decrease in the number of $CD4^+CD25^+$ T cells may be one of the mechanisms leading to immune dysregulation in immune thrombocytopenia (ITP), and the changes in the number of $CD4^+CD25^+$ T cells are considered to be associated with the severity of ITP (25). The lack of $CD4^+CD25^+$ T cells can lead to severe autoimmune/inflammatory diseases, while normal regulatory T cells (Tregs) can inhibit disease development (50). CD122 is the β subunit of the IL-2 receptor, not only regulating Tregs but also influencing Treg function. $CD8^+CD122^+$ T cells may regulate immune responses by producing IL-10, TGFβ1 and IFNγ; however, the exact mechanism of their inhibitory effect remains largely unknown (51,52). Previous studies have indicated that $CD8^+CD122^+$ T cells could suppress T cell responses, modulated autoimmunity and alloimmune responses, and served an important role in autoimmune diseases (52-54). The development of systemic lupus erythematosus-like disease in B6-Yaa mutant mice is associated with a defect in $CD8^+CD122^+$ T cells (55). Disruption of the inhibitory interaction between $CD8^+CD122^+$ T cells and follicular helper T cells leads to the development of a lethal systemic lupus erythematosus-like autoimmune disease dependent on autoantibodies (56). The depletion of $CD8^+CD122^+$ T cells increases the incidence of AITD (57). Research data show that $CD8^+CD122^+$ T cells in secondary lymphoid organs of prediabetic non-obese diabetic mice are reduced by ~50%, highlighting the role of $CD8^+CD122^+$ T cells in suppressing autoimmune diseases (26). Several studies have shown that $CD4^+CD25^+$ and $CD8^+CD122^+$ T cells serve a key role in the incidence and severity of GD, HT and hypothyroidism (57,58). The present study revealed that immunization with hTSHR fusion protein led to a decrease in the number of $CD4^+CD25^+$ and $CD8^+CD122^+$ T cells in the secondary lymphoid organs of

mice. Collectively, the data in the present study suggested that the three types of TSHR fusion proteins that were prepared could induce immune dysregulation in BALB/c mice, leading to the development of AITD.

The present study offers insights into the significance of different structural domains of TSHR in the pathogenesis of AITD. Additionally, the TRAb assay kit may also be used to monitor changes in the condition of patients, providing evidence for the early diagnosis and individualized treatment of patients. The primary concern now is that the ELISA may face issues when used in clinical testing, such as false positives, and low sensitivity and specificity, which will affect the diagnosis and treatment of patients. Therefore, multi-center and large-sample research and testing are required, which should include a larger group of patients. A more stable and accurate ELISA detection system also needs to be created to improve reliability and clinical applicability. In the present study, three fusion proteins were prepared according to the characteristics of the TSHR domain, and the regions that TSHR may bind with TSAb and TBAb were initially identified. In the subsequent experiment, the extracellular region of TSHR was segmented into smaller structural units according to the structural characteristics of the internal functional characteristics of a single domain. Further refining and clarifying the binding sites of TSAb, TBAb and TSHR is also an effective way of reducing false positives and increasing sensitivity and specificity. In addition, combining the fusion protein with TRAb detection methods such as the current third-generation TBII method and biological assays is also one of the methods for more accurate diagnosis and treatment of patients, which needs further research.

Therefore, a comprehensive understanding of the biological effects of the TSHR fusion protein and in-depth exploration of the specific mechanism of TSHR fusion protein inducing the immune response can help increase the understanding of the pathogenesis of AITD, provides a scientific basis for research of TSHR and the application of fusion proteins, and provides a basis for the accurate diagnosis, and individualized diagnosis and treatment of patients with AITD.

In view of the important role of TSHR in AITDs, the present study expressed fusion proteins of different domains of TSHR, and the fusion proteins of different domains of TSHR exhibited different immunogenicity. The TSHR A subunit fusion protein and TSHR carboxyl-terminal fusion protein prepared in the present study could serve as a basis for the development of ELISA kits for the detection of TSAb and TBAb. Fusion proteins of different structural domains of TSHR induced clinical symptoms of hyperthyroidism and hypothyroidism in mice. This research provides a scientific basis for future studies on the etiology and mechanisms of AITD, as well as the invention of novel methods for the detection of TRAb.

Acknowledgements

Not applicable.

Funding

The present study was supported by the Science and Technology Plan Project of Gansu Province (Basic Research Plan; grant no. 25JRRA597) and the Lanzhou University Second Hospital 'Cuiying Technological Innovation' Program (grant no. CY2018-ZD02).

Availability of data and materials

The data generated in the present study may be requested from the corresponding author.

Authors' contributions

XC contributed to conceptualization, methodology,-visualization, writing of the original draft and editing. HC contributed to conceptualization, acquired funding, provided resources, supervised the study and revised the manuscript. Both authors have read and approved the final version of the manuscript. XC and HC confirm the authenticity of all the raw data.

Ethics approval and consent to participate

The animal experiments received approval from the Animal Welfare and Ethics Committee of The Second Hospital of Lanzhou University (approval no. D2023-156; Lanzhou, China). The research protocol was reviewed and approved by the Medical Ethics Committee of The Second Hospital of Lanzhou University (approval no. 2023A-802; Lanzhou, China). All participants provided written informed consent prior to participating in the present study. All experiments have been approved by the appropriate ethics committee and have therefore been performed in accordance with the ethical standards laid down in the 1964 Declaration of Helsinki and its later amendments.

Patient consent for publication

Informed consent from patients was obtained for publication of the present study, and relevant written consent has been provided.

Competing interests

The authors declare that they have no competing interests.

References

1. McLachlan SM and Rapoport B: Thyroid autoantibodies display both 'Original antigenic sin' and epitope spreading. Front Immunol 8: 1845, 2017.
2. Furmaniak J, Sanders J, Núñez Miguel R and Rees Smith B: Mechanisms of action of TSHR autoantibodies. Horm Metab Res 47: 735-752, 2015.
3. Furmaniak J, Sanders J, Sanders P, Li Y and Rees Smith B: TSH receptor specific monoclonal autoantibody K1-70™ targeting of the TSH receptor in subjects with Graves' disease and Graves' orbitopathy-Results from a phase I clinical trial. Clin Endocrinol (Oxf) 96: 878-887, 2022.
4. Gupta AK and Kumar S: Utility of antibodies in the diagnoses of thyroid diseases: A review article. Cureus 14: e31233, 2022.
5. Smith TJ and Hegedüs L: Graves' disease. N Engl J Med 375: 1552-1565, 2016.
6. Latif R, Mezei M, Morshed SA, Ma R, Ehrlich R and Davies TF: A Modifying autoantigen in Graves' disease. Endocrinology 160: 1008-1020, 2019.
7. Núñez Miguel R, Sanders P, Allen L, Evans M, Holly M, Johnson W, Sullivan A, Sanders J, Furmaniak J and Rees Smith B: Structure of full-length TSH receptor in complex with antibody K1-70™. J Mol Endocrinol 70: e220120, 2022.

8. George A, Diana T, Längericht J and Kahaly GJ: Stimulatory thyrotropin receptor antibodies are a biomarker for graves' orbitopathy. Front Endocrinol (Lausanne) 11: 629925, 2021.
9. Lytton SD, Schluter A and Banga PJ: Functional diagnostics for thyrotropin hormone receptor autoantibodies: Bioassays prevail over binding assays. Front Biosci (Landmark Ed) 23: 2028-2043, 2018.
10. Bahn RS: Current Insights into the Pathogenesis of Graves' Ophthalmopathy. Horm Metab Res 47: 773-778, 2015.
11. Faßbender J, Holthoff HP, Li Z and Ungerer M: Therapeutic effects of short cyclic and combined epitope peptides in a Long-term model of Graves' disease and orbitopathy. Thyroid 29: 258-267, 2019.
12. Rapoport B, Aliesky HA, Chen CR and McLachlan SM: Evidence that TSH receptor A-subunit multimers, not monomers, drive antibody affinity maturation in Graves' disease. J Clin Endocrinol Metab 100: E871-E875, 2015.
13. Li CW, Osman R, Menconi F, Concepcion E and Tomer Y: Cepharanthine blocks TSH receptor peptide presentation by HLA-DR3: Therapeutic implications to Graves' disease. J Autoimmun 108: 102402, 2020.
14. Holthoff HP, Goebel S, Li Z, Faßbender J, Reimann A, Zeibig S, Lohse MJ, Münch G and Ungerer M: Prolonged TSH receptor A subunit immunization of female mice leads to a long-term model of Graves' disease, tachycardia, and cardiac hypertrophy. Endocrinology 156: 1577-1589, 2015.
15. Rapoport B, Chazenbalk GD, Jaume JC and McLachlan SM: The thyrotropin (TSH) receptor: Interaction with TSH and autoantibodies. Endocr Rev 19: 673-716, 1998.
16. Davies TF, Ando T, Lin RY, Tomer Y and Latif R: Thyrotropin receptor-associated diseases: From adenomata to Graves disease. J Clin Invest 115: 1972-1983, 2005.
17. Latif R, Teixeira A, Michalek K, Ali MR, Schlesinger M, Baliram R, Morshed SA and Davies TF: Antibody protection reveals extended epitopes on the human TSH receptor. PLoS One 7: e44669, 2012.
18. Marcinkowski P, Kreuchwig A, Mendieta S, Hoyer I, Witte F, Furkert J, Rutz C, Lentz D, Krause G and Schülein R: Thyrotropin receptor: Allosteric modulators illuminate intramolecular signaling mechanisms at the interface of Ecto- and transmembrane domain. Mol Pharmacol 96: 452-462, 2019.
19. Thyroid disease: Assessment and management. London, National Institute for Health and Care Excellence (NICE), November 20, 2019.
20. Holthoff HP, Uhland K, Kovacs GL, Reimann A, Adler K, Wenhart C and Ungerer M: Thyroid-stimulating hormone receptor (TSHR) fusion proteins in Graves' disease. J Endocrinol 246: 135-147, 2020.
21. Yang Y, Xia Q, Zhou L, Zhang Y, Guan Z, Zhang J, Li Z, Liu K, Li B, Shao D, *et al*: B602L-Fc fusion protein enhances the immunogenicity of the B602L protein of the African swine fever virus. Front Immunol 14: 1186299, 2023.
22. Percie du Sert N, Hurst V, Ahluwalia A, Alam S, Avey MT, Baker M, Browne WJ, Clark A, Cuthill IC, Dirnagl U, *et al*: The ARRIVE guidelines 2.0: Updated guidelines for reporting animal research. PLoS Biol 18: e3000410, 2020.
23. Zheng H, Xu J, Chu Y, Jiang W, Yao W, Mo S, Song X and Zhou J: A global regulatory network for dysregulated gene expression and abnormal metabolic signaling in immune cells in the microenvironment of Graves' disease and Hashimoto's thyroiditis. Front Immunol 13: 879824, 2022.
24. Kristensen B: Regulatory B and T cell responses in patients with autoimmune thyroid disease and healthy controls. Dan Med J 63: B5177, 2016.
25. Hsu WT, Suen JL and Chiang BL: The role of CD4CD25 T cells in autoantibody production in murine lupus. Clin Exp Immunol 145: 513-519, 2006.
26. Arndt B, Witkowski L, Ellwart J and Seissler J: CD8+ CD122+ PD-1-effector cells promote the development of diabetes in NOD mice. J Leukoc Biol 97: 111-120, 2015.
27. Benvenga S, Elia G, Ragusa F, Paparo SR, Sturniolo MM, Ferrari SM, Antonelli A and Fallahi P: Endocrine disruptors and thyroid autoimmunity. Best Pract Res Clin Endocrinol Metab 34: 101377, 2020.
28. Taylor PN, Albrecht D, Scholz A, Gutierrez-Buey G, Lazarus JH, Dayan CM and Okosieme OE: Global epidemiology of hyperthyroidism and hypothyroidism. Nat Rev Endocrinol 14: 301-316, 2018.
29. Duan J, Xu P, Cheng X, Mao C, Croll T, He X, Shi J, Luan X, Yin W, You E, *et al*: Structures of full-length glycoprotein hormone receptor signalling complexes. Nature 598: 688-692, 2021.
30. Jiang X, Liu H, Chen X, Chen PH, Fischer D, Sriraman V, Yu HN, Arkinstall S and He X: Structure of follicle-stimulating hormone in complex with the entire ectodomain of its receptor. Proc Natl Acad Sci USA 109: 12491-12496, 2012.
31. Kleinau G, Mueller S, Jaeschke H, Grzesik P, Neumann S, Diehl A, Paschke R and Krause G: Defining structural and functional dimensions of the extracellular thyrotropin receptor region. J Biol Chem 286: 22622-22631, 2011.
32. Rapoport B and McLachlan SM: TSH receptor cleavage into subunits and shedding of the A-subunit; a molecular and clinical perspective. Endocr Rev 37: 114-134, 2016.
33. Couët J, de Bernard S, Loosfelt H, Saunier B, Milgrom E and Misrahi M: Cell surface protein disulfide-isomerase is involved in the shedding of human thyrotropin receptor ectodomain. Biochemistry 35: 14800-14805 1996.
34. Duan J, Xu P, Luan X, Ji Y, He X, Song N, Yuan Q, Jin Y, Cheng X, Jiang H, *et al*: Hormone- and antibody-mediated activation of the thyrotropin receptor. Nature 609: 854-859, 2022.
35. Faust B, Billesbølle CB, Suomivuori CM, Singh I, Zhang K, Hoppe N, Pinto AFM, Diedrich JK, Muftuoglu Y, Szkudlinski MW, *et al*: Autoantibody mimicry of hormone action at the thyrotropin receptor. Nature 609: 846-853, 2022.
36. Morshed SA and Davies TF: Graves' disease mechanisms: The role of stimulating, blocking, and cleavage region TSH receptor antibodies. Horm Metab Res 47: 727-734, 2015.
37. Akamizu T, Kosugi S, Kohn LD and Mori T: Anti-thyrotropin (TSH) receptor antibody binding epitopes of TSH receptor: Site-directed mutagenesis approach. Nihon Rinsho 52: 1024-1030, 1994 (In Japanese).
38. Zulkarnain Z, Ulhaq ZS, Sujuti H, Soeatmadji DW, Zufry H, Wuragil DK, Marhendra APW, Riawan W, Kurniawati S, Oktanella Y and Aulanni'am A: Comparative performance of ELISA and dot blot assay for TSH-receptor antibody detection in Graves' disease. J Clin Lab Anal 36: e24288, 2022.
39. McLachlan SM, Aliesky HA, Garcia P, Banuelos B and Rapoport B: Thyroid hemiagenesis in a thyroiditis prone mouse strain. Eur Thyroid J 7: 187-192, 2018.
40. Rapoport B, Aliesky HA, Banuelos B, Chen CR and McLachlan SM: A unique mouse strain that develops spontaneous, Iodine-accelerated, pathogenic antibodies to the human thyrotrophin receptor. J Immunol 194: 4154-4161, 2015.
41. Schlüter A, Horstmann M, Diaz-Cano S, Plöhn S, Stähr K, Mattheis S, Oeverhaus M, Lang S, Flögel U, Berchner-Pfannschmidt U, *et al*: Genetic immunization with mouse thyrotrophin hormone receptor plasmid breaks Self-tolerance for a murine model of autoimmune thyroid disease and Graves' orbitopathy. Clin Exp Immunol 191: 255-267, 2018.
42. Porowińska D, Wujak M, Roszek K and Komoszyński M: Prokaryotic expression systems. Postepy Hig Med Dosw (Online) 67: 119-129, 2013 (In Polish).
43. Costagliola S, Alcalde L, Tonacchera M, Ruf J, Vassart G and Ludgate M: Induction of thyrotropin receptor (TSH-R) autoantibodies and thyroiditis in mice immunised with the recombinant TSH-R. Biochem Biophys Res Commun 199: 1027-1034, 1994.
44. Janyga S, Marek B, Kajdaniuk D, Ogrodowczyk-Bobik M, Urbanek A and Bułdak Ł: CD4+ cells in autoimmune thyroid disease. Endokrynol Pol 72: 572-583, 2021.
45. Yin L, Zeng C, Yao J and Shen J: Emerging roles for noncoding RNAs in autoimmune thyroid disease. Endocrinology 161: bqaa053, 2020.
46. Sakaguchi S, Mikami N, Wing JB, Tanaka A, Ichiyama K and Ohkura N: Regulatory T cells and human disease. Annu Rev Immunol 38: 541-566, 2020.
47. Grindebacke H, Wing K, Andersson AC, Suri-Payer E, Rak S and Rudin A: Defective suppression of Th2 cytokines by CD4CD25 regulatory T cells in birch allergics during birch pollen season. Clin Exp Allergy 34: 1364-1372, 2004.
48. Rosenberger S, Undeutsch R, Akbarzadeh R, Ohmes J, Enghard P, Riemekasten G and Humrich JY: Regulatory T cells inhibit autoantigen-specific CD4+ T cell responses in lupus-prone NZB/W F1 mice. Front Immunol 14: 1254176, 2023.
49. Yan JJ, Lee JG, Jang JY, Koo TY, Ahn C and Yang J: IL-2/anti-IL-2 complexes ameliorate lupus nephritis by expansion of CD4+CD25+Foxp3+ regulatory T cells. Kidney Int 91: 603-615, 2017.
50. Malek TR and Castro I: Interleukin-2 receptor signaling: At the interface between tolerance and immunity. Immunity 33: 153-165, 2010.

51. Rifa'i M, Kawamoto Y, Nakashima I and Suzuki H: Essential roles of CD8+CD122+ regulatory T cells in the maintenance of T cell homeostasis. J Exp Med 200: 1123-1134, 2004.
52. Yuan X, Dong Y, Tsurushita N, Tso JY and Fu W: CD122 blockade restores immunological tolerance in autoimmune type 1 diabetes via multiple mechanisms. JCI Insight 3: e96600, 2018.
53. Liu J, Chen D, Nie GD and Dai Z: CD8(+)CD122(+) T-cells: A newly emerging regulator with central memory cell phenotypes. Front Immunol 6: 494, 2015.
54. Mishra S, Srinivasan S, Ma C and Zhang N: CD8+ regulatory T cell-a mystery to be revealed. Front Immunol 12: 708874, 2021.
55. Kim HJ, Wang X, Radfar S, Sproule TJ, Roopenian DC and Cantor H: CD8+ T regulatory cells express the Ly49 Class I MHC receptor and are defective in autoimmune prone B6-Yaa mice. Proc Natl Acad Sci USA 108: 2010-2015, 2011.
56. Kim HJ, Verbinnen B, Tang X, Lu L and Cantor H: Inhibition of follicular T-helper cells by CD8(+) regulatory T cells is essential for self tolerance. Nature 467: 328-332, 2010.
57. Saitoh O, Abiru N, Nakahara M and Nagayama Y: CD8+CD122+ T cells, a newly identified regulatory T subset, negatively regulate Graves' hyperthyroidism in a murine model. Endocrinology 148: 6040-6046, 2007.
58. McLachlan SM, Nagayama Y, Pichurin PN, Mizutori Y, Chen CR, Misharin A, Aliesky HA and Rapoport B: The link between Graves' disease and Hashimoto's thyroiditis: A role for regulatory T cells. Endocrinology 148: 5724-5733, 2007.